2021 60th IEEE Conference on Decision and Control (CDC)
December 13-15, 2021. Austin, Texas

2021 60th IEEE Conference on Decision and Control (CDC) | 978-1-6654-3659-5/21/$31.00 ©2021 IEEE | DOI: 10.1109/CDC45484.2021.9683312

Accommodation of Pulsed Field Gradients with Cascade Field Regulation in Powered Magnets

Benjamin D. McPheron*†, Jeffrey L. Schiano†, Ilya M. Litvak‡, William W. Brey ‡
*School of Science and Engineering
Anderson University, Anderson, Indiana 46012
Email: bdmcpheron@anderson.edu
†School of Electrical Engineering and Computer Science
The Pennsylvania State University, University Park, PA 16802
‡National High Magnetic Field Laboratory, Florida State University, Tallahassee, Florida 32310

***Abstract*—High magnetic fields significantly improve the resolution and sensitivity of nuclear magnetic resonance (NMR) spectroscopy measurements, which presents exciting research opportunities in areas of chemistry, biology, and material science. Powered magnets can provide much higher magnetic fields than persistent mode superconducting magnets but suffer from temporal magnetic field fluctuations due to power supply ripple and variations in cooling water temperature and flow rate which make powered magnets non-viable for high resolution NMR experiments. Previous work has demonstrated that a multi-rate sampled data cascade control system may be used to improve the resolution of NMR experiments in powered magnets. Despite these advances in reducing temporal magnetic field fluctuations, the field regulation design does not accommodate the use of pulsed field gradients, which are necessary in many NMR experiments. This work presents a control topology which accommodates the use of pulsed field gradient signals with the field regulation system. This control approach is verified using NMR measurements.**

I. Introduction

Powered magnets are capable of producing high fields that can dramatically improve magnetic resonance (MR) spectroscopy measurements, which includes both nuclear magnetic resonance (NMR) and magnetic resonance imaging (MRI) experiments. However, temporal magnetic field fluctuations introduced into powered magnets by power supply ripple and variations in temperature and flow rate of the cooling water systems make powered magnets infeasible for high resolution MR measurements [1].

Previous work has shown that multi-rate sampled data feedback control can be applied to reduce field variation in powered magnets to allow for high resolution MR experiments [2], [3]. The proposed feedback system, shown in Figure 1, is composed of a fast inner loop sampled at 50 kHz and a slow outer loop sampled at 40 Hz. The inner loop uses an inductive sensor and is designed to correct high frequency temporal field fluctuations arising from power supply ripple, while the outer loop employs an NMR frequency estimator and is designed to correct low frequency field fluctuations due to variations in cooling water temperature and flow rate.

The inner loop controller $G_{Ci}(s)$ is the series combination of a proportional gain K, a 4th order phase-lead-lag compensator ($G_{PLL}(s)$), and four 2nd order notch filters ($G_{IMP}(s)$) which cancel harmonics of 60 Hz. In other words,

$$G_{Ci}(s) = KG_{PLL}(s)G_{IMP}(s). \tag{1}$$

The outer loop controller $G_{Co}(s)$ is composed of the phase-lag compensator

$$G_{PL}(s) = 1000\left(\frac{\frac{s}{2\pi 0.5}+1}{\frac{s}{2\pi 0.05}+1}\right)\left(\frac{\frac{s}{2\pi 10}+1}{\frac{s}{2\pi 1}+1}\right) \tag{2}$$

in parallel with a derivative term

$$G_D(s) = 10\left(\frac{s}{s+1}\right). \tag{3}$$

$G_{Ci}(z)$ and $G_{Co}(z)$ are the zero-order hold equivalents of their continuous time counterparts, sampled at 50 kHz and 40 Hz, respectively [3].

The improvement afforded by this regulation system is demonstrated in Figure 2, which shows the peak frequency for a set of 128 consecutive excitations. With no compensation, the peak frequencies shift by 4.97 G (1.43 Grms). With inner loop compensation only, the peak frequencies shift by 1.66 G (0.528 Grms). With the cascade control configuration, the field is further improved to a shift of less than 48.7 mG (9.80 mGrms).

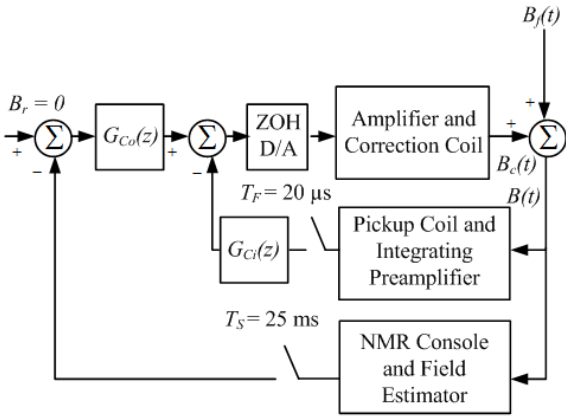

Fig. 1. Cascade field regulation system [3].

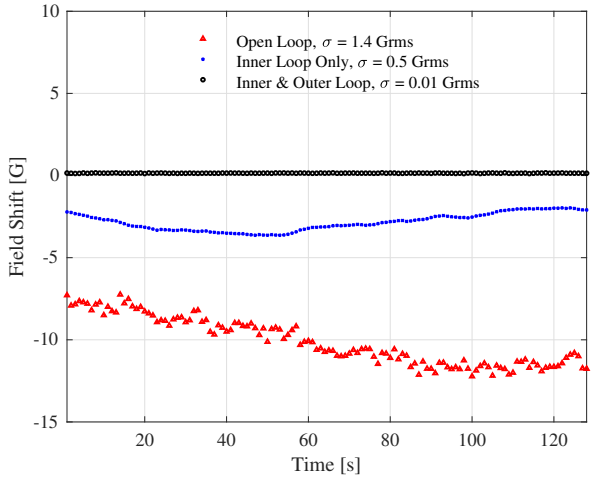

Fig. 2. Spectral peak locations for a series of free induction decay experiments in the Keck powered magnet at 25 T [3].

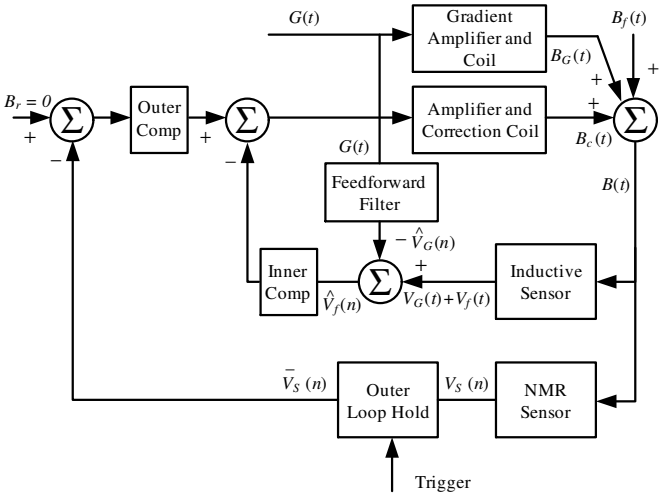

Fig. 3. Block diagram representing the gradient correction concept and placement in the cascade regulation system.

Many classes of high resolution MR experiments, such as diffusion measurements, magnetic resonance imaging (MRI), and solvent suppression require the use of pulsed field gradients to introduce a spatially varying magnetic field [4], [5], [6], [7]. However, the operation of the cascade field regulation system is negatively affected by pulsed field gradients in two ways: (1) the inner loop inductive sensor measures pulsed field gradient signals; (2) the NMR signal used by the outer loop field estimator is spoiled when a gradient signal is pulsed and the reported estimate is incorrect. These inaccurate measures of field fluctuations result in spurious controller response in both the inner and outer loop, which attempt to attenuate the spatially varying magnetic field from the gradient signal and inadvertently introduce new field fluctuations. The controller response to the pulsed field gradient signals renders it impossible to perform MR experiments employing pulsed field gradients simultanesouly with the field regulation system [1].

This paper presents an updated control strategy which accommodates pulsed field gradients with both the outer loop and inner loop field regulation subsystems. The outer loop gradient correction scheme is implemented as an estimate hold, which ignores the NMR signals that arise in error when pulsed field gradients are applied. The inner loop employs a feedforward correction filter to remove the gradient signal from the inductive measurements.

This work was completed as part of the control system development for the 36 T Series-Connected Hybrid magnet now in operation at the National High Magnetic Field Laboratory (NHMFL) in Tallahassee, Florida [8]. The NHMFL is a shared-user facility, and each experimental run is limited to a power allotment for completion of experiments due to the high cost of running powered magnets at full field. As this is the case, much of the development and verification of the gradient correction techniques presented in the previous section were tested on a readily available 7.1 T superconducting magnet with injected field fluctuations.

II. Gradient Correction Control Design

Pulsed field gradients affect both the outer loop and inner loop subsystems of the cascade regulation system as described in Section I. As a result, it was necessary to develop correction schemes to accommodate pulsed field gradients in both subsystems. A block diagram of the control system with the outer loop gradient hold and inner loop feedforward gradient correction integrated into the cascade regulation system is presented in Figure 3. The outer loop gradient correction scheme is implemented by an estimate hold which has two inputs: a gradient trigger and the field estimate. For inner loop gradient correction, a feedforward filter is used with an input of the commanded gradient signal.

A. Outer Loop Gradient Hold

When a gradient occurs, it spoils the free induction decay data needed for field estimation. This means that the following estimate will be in error. Figure 4 illustrates the effect of a train of field gradient pulses on the outer loop estimation system. Here, a 0.1 Hz ramp disturbance was injected into the 7.1 T persistent superconducting magnet. In addition, a train of 50 G/cm gradient pulses, each with duration 6 ms, was applied to simulate the type of pulses that are needed in a practical NMR experiment. The spikes present are due to the estimation error occuring when the gradient pulses are applied.

To demonstrate the effect of the gradient signal on the outer loop estimation system consider Figure 4, which shows a 0.1 Hz ramp disturbance injected into the 7.1 T persistent superconducting magnet with a 50 G/cm gradient periodically applied. This data shows the estimation error corresponding to gradient signals.

The estimate at the sample time immediately before the gradient pulse is held for the duration of the gradient (typically on the order of milliseconds) so that the gradient signal does

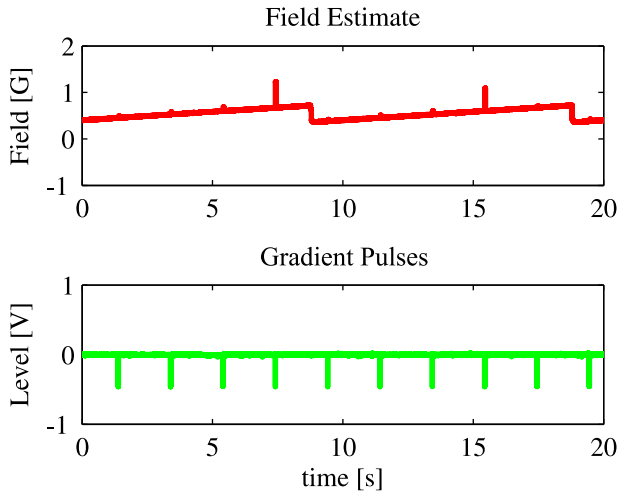

Fig. 4. Field estimate of outer loop in the presence of ramp disturbance and a gradient pulse train. The spikes indicate errors in the field estimate caused by the gradient pulse train.

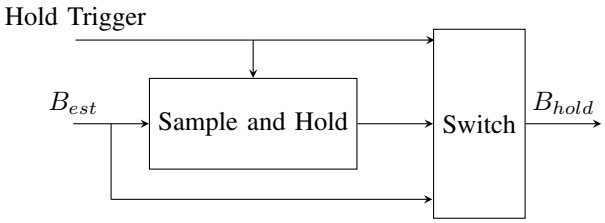

Fig. 5. Outer loop gradient hold scheme.

not result in incorrect estimation. Since the field estimator is designed to measure slow fluctuations below 20 Hz (≥a 50 ms period), the error in estimate is relatively small. The gradient hold ensures that the estimate from before the gradient signal is held through the current estimator sample time and through the next update. Otherwise, the field estimate B_{est} passes as normal. The result is a field estimate B_{hold} that ignores gradient signals. Figure 5 shows the block diagram of the outer loop gradient hold implementation.

Figure 6 shows the field estimate with gradient hold system operating. A "hold trigger" of the appropriate duration is generated for each gradient pulse. The estimate now correctly follows the ramp signal but ignores the gradient signals.

B. Feedforward Gradient Correction

Because the inductive field sensor is never exactly lined up with the center of the field gradient coils, field gradient pulses induce an error signal in the inductive sensor. The field regulation system will then attempt to correct the error, producing a magnetic field resulting in an unwanted shift in NMR frequency.

Figure 7 shows both the field estimate with the gradient hold activated, as well as the output of the inductive measurement system, which has clear gradient signal peaks.

A feedforward filter is used to remove gradient signals from the inductive measurement fed into the inner loop controller. Figure 8 shows a block diagram of the feedforward filter

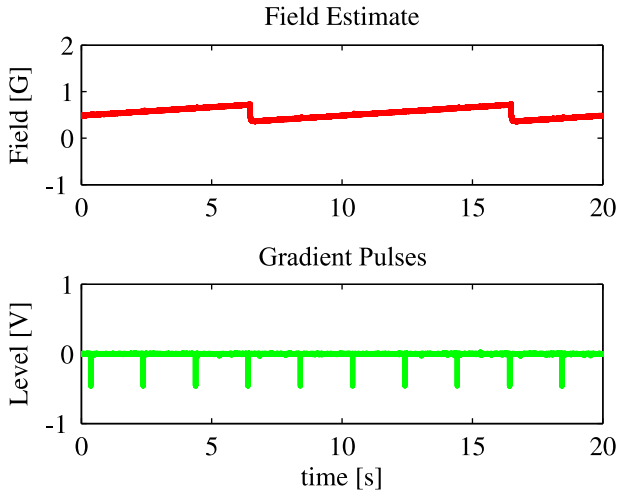

Fig. 6. Field estimate with ramp and gradients applied with outer loop hold activated.

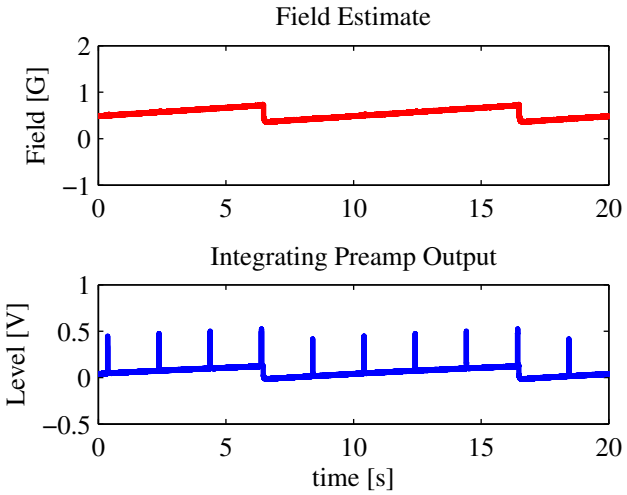

Fig. 7. Field estimate and inductive measurement with outer loop hold activated.

configuration used for gradient correction in the inner loop. In this configuration, a gradient signal $G(t)$ is applied to the system. The gradient signal drives the gradient amplifier and gradient coil, inducing a time dependent magnetic field $B_G(t)$ which is added to the time varying magnetic field fluctuations in a powered magnet $B_f(t)$, yielding a net field $B(t)$, which is measured as $V_f(t)$ + $V_G(t)$ by the inductive sensor.

The feedforward filter estimates the measured voltage $\hat{V}_G(t)$ of the gradient signal. This estimate, $\hat{V}_G(t)$, is subtracted from the inductive sensor measurement $V_f(t)$ + $V_G(t)$, yielding an estimate $\hat{V}_f(t)$ of the field fluctuation measurement $V_f(t)$, which can be used as the input to the inner loop compensator.

In practice, the feedforward filter and summation are performed in a digital signal processor, which implements the filter in discrete time. System identification using the Output Error Method was found to minimize the error between the estimated response and the measured response of the inductive measurement system [9]. The identified filter transfer function

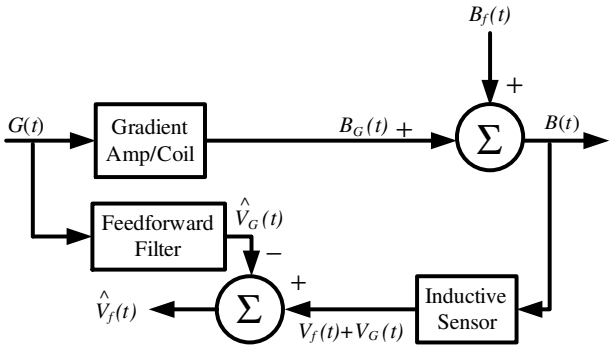

Fig. 8. Feedforward filter to remove gradient component.

is

$$G_{FF}(z) = \frac{-0.096z^3 + 0.11z^2 - 0.015z}{z^4 - 1.331z^3 - 0.509z^2 + 1.121z - 0.281} \quad (4)$$

which is a stable, causal system.

To demonstrate that both the gradient hold and feedforward gradient correction schemes successfully accommodate pulsed field gradient signals with the cascade control system, a 0.1 Hz ramp signal was again injected into the 7.1 T superconducting magnet while 50 G/cm gradient signals were periodically applied. Figure 9 shows that both the field estimator and the inductive measurement track the ramp disturbance and gradient signals do not cause large errors in the measurement.

III. MR Performance Metrics

In order to evaluate the performance of the gradient correction schemes employed in this work, three MR metrics were used.

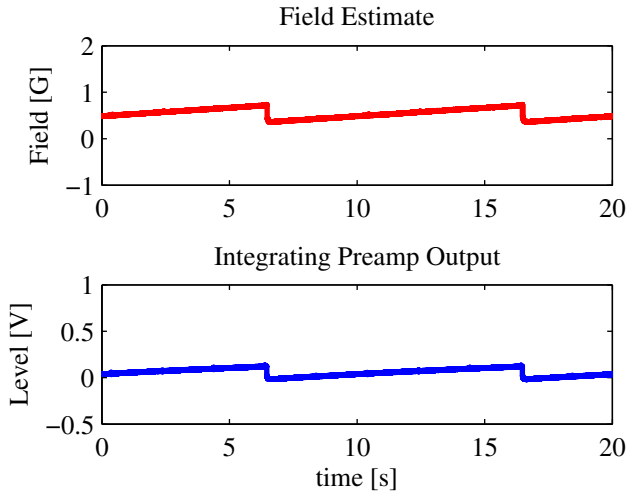

Fig. 9. Ramp and gradients applied with full gradient correction scheme activated

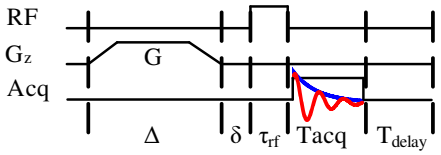

Fig. 10. Pulse sequence used to produce gradient augmented NMR excitation signals.

To obtain the first two metrics, we set up a worst-case experiment: a NMR excitation immediately following a field gradient pulse. We then recorded the frequency and spectral lineshape of the NMR response. The frequency of the response is directly proportional to the time average of the magnetic field seen by the sample. In contrast, the lineshape provides a qualitative indication of the change in field that occurs during the NMR response. The observed change in the location of the spectral peak of among the successive excitation signals provides a quantitative metric for assessing the slow temporal drift of the magnetic field due to variation in the flow rate and temperature of cooling water. The spectrum has a Lorentzian lineshape in the absence of field fluctuations, but when temporal magnetic field fluctuations are introduced, the lineshape is broadened. Erroneous control signals attempting to correct for detected gradient signals will also distort the lineshape, which is why both peak frequency and lineshape are assessed. The pulse sequence employed to trigger this response is shown in Figure 10. The pulse parameters used were δ=1 μs, G=80 G/cm, Δ=6 ms, and T_{delay}=1 s. The acquisition time $Tacq$ was 16.384 ms in the 7.1 T persistent superconducting magnet, and 1.024 ms in the Keck powered magnet at 25 T.

The last MR metric used is the standard deviation spin echo phase ($\sigma_{SE}(T_E)$) [2]. In this test, a series of spin echo signals are recorded. The presence of temporal field fluctuations causes the phase at the echo center to vary from trial to trial. In the absence of field fluctuations, such as in a persistent superconducting magnet, the phase at echo center is the same across repeated trials, and $\sigma_{SE}(T_E)$ of the measured phase approaches zero. As field fluctuation magnitude increases, $\sigma_{SE}(T_E)$ also increases, providing a good measure of temporal field fluctuations [2]. This is measured at several echo times (T_E), with at least 100 measurements per T_E.

To evaluate the performance of the gradient correction control approach, the spin echo sequence can be augmented by the application of a pulsed field gradient signal directly before the sequence. The controller transient response to pulsed field gradient signals occurs on the order of milliseconds and the T_E values used to measure the standard deviation of spin echo phase are also on the order of milliseconds, so this metric provides a reasonable measure of gradient correction performance. The pulse sequence used to generate a spin echo response is shown in Figure 11. A gradient signal is activated directly before the first RF pulse of the spin echo sequence, to ensure that the controller transient response to a gradient

signal will occur during the spin echo acquisition window providing a measure of gradient correction performance. The pulse parameters used were δ=1 μs, G=80 G/cm, Δ=6 ms, T_{delay}=3 s, $Tacq$=16.384 ms, τ_{90}=115 μs and τ_{180}=230 μs in the 7.1 T persistent superconducting magnet.

In the case of no feedback control, $\sigma_{SE}(T_E)$ will be very large at all T_E values. The application of the field regulation system will greatly reduce $\sigma_{SE}(T_E)$, even with spurious control signals due pulsed field gradients. To verify the performance of the gradient correction control strategy, $\sigma_{SE}(T_E)$ with and without gradient correction is compared. Without gradient correction, the controller transient response to the gradient signal introduces new field fluctuations, perturbing the MR signal and increasing $\sigma_{SE}(T_E)$. If the gradient correction scheme is effective, results should display a marked decrease in the standard deviation for all T_E values.

IV. NMR Verification of Gradient Correction Control

Two magnet testbeds are used in this work: the 25 T Keck powered magnet and a 7.1 T superconducting magnet with field fluctuations recorded from the Keck powered magnet injected to simulate the powered magnet environment.

A. Gradient Augmented NMR Excitation: Spectral Peak Frequency and Lineshape

The first MR metric used was spectral peak frequency measurements and lineshape for the gradient augmented NMR excitation pulse sequence described in Section III. The results of this experiment in the 7.1 T superconducting magnet are shown in Figure 12. which shows a series of 100 g-FIDs collapsed into a 2D plane where the frequency indicates relative difference from NMR console measurement set-point for a ^{1}H signal (approximately 300 MHz at 7.1 T). In Figure 12 (A), the data show significant field variation as expected from a powered magnet environment, which is provided by the injected Keck disturbance. The NMR signal varies frequency location between consecutive experiments due to the fast fluctuations introduced in powered magnets by power supply ripple. The NMR signal also slowly drifts in the frequency domain due to the slow drift from cooling water temperature and flow rate variations.

By activating the cascade field regulation system, the field variations are significantly reduced, and thus subsequent scans appear to sit on top of each other in 2D view. However, with no gradient correction, the response to pulsed field gradient signals introduces significant distortion to the NMR signal. Figure 12 (B) shows the reduction in variations, as well as the distorted lineshape. The frequency variation is significantly reduced from the variations in the open loop case, but the distorted lineshape and attenuated gradient signal require correction.

With gradient correction control, the lineshape improves. Figure 12 (C) shows that the lineshape is no longer distorted by the controller response to the pulsed field gradient signal. This result shows that the gradient correction scheme, including feedforward gradient correction and outer loop gradient hold, can be applied to allow the use of pulsed field gradients with the cascade field regulation system.

The spectral peak frequency variation is reduced from 1.3 G rms in the open loop case to 16 mG rms when the cascade regulation system with gradient correction is activated, am improvment of around 38 dB. The lineshape also appears more Lorentzian with gradient correction control than it does without.

As further demonstration of the lineshape improvement provided by the gradient correction scheme, a similar experiment was repeated in the Keck powered magnet at 25 T. Figure 13 shows the lineshape from a single gradient augmented NMR excitation in the powered magnet. In particular, comparing the lineshape in Figure 13 (B) with no gradient correction to the lineshape in Figure 13 (C) with gradient correction, there is a significant reduction in lineshape distortion, indicating that the effect of gradients on the signal is significantly reduced, to the point that it appears the same as (A) on this scale.

B. Standard Deviation of Spin Echo Phase with Gradients

The other metric applied was finding the standard deviation of gradient-spin echo phase. In this experiment, $\sigma_{SE}(T_E)$ is measured for a series of 100 spin echoes at varying T_E values.

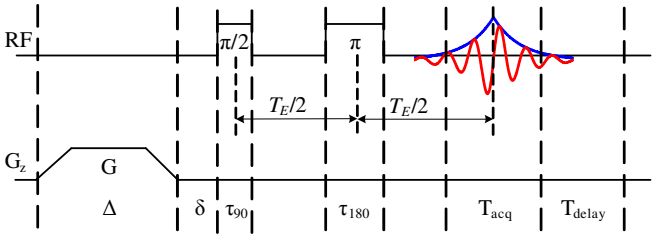

Fig. 11. Spin echo with gradient MR pulse sequence.

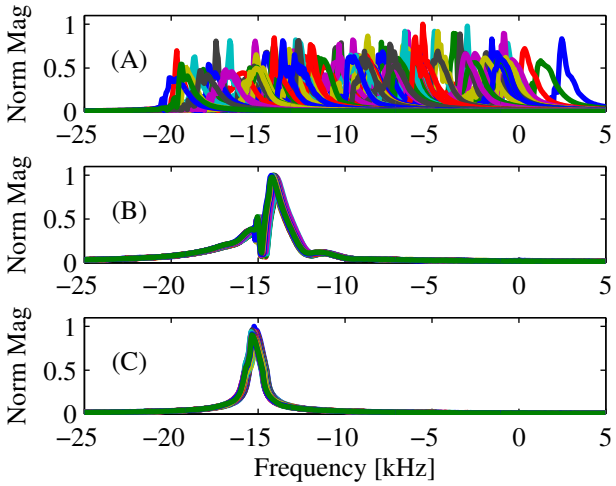

Fig. 12. Series of 100 gradient augmented NMR excitation experiments with powered magnet disturbance applied with (A) no regulation (B) cascade field regulation with no gradient correction and (C) cascade field regulation with gradient correction.

Figure 14 shows these results for T_E values ranging from 5 ms to 30 ms. With no regulation applied, $\sigma_{SE}(T_E)$ is large for all T_E values. Applying field regulation reduces these values, and adding gradient correction further reduces $\sigma_{SE}(T_E)$ by lowering controller response to pulsed field gradient signals. It can be seen that $\sigma_{SE}(T_E)$ is lower at all values of T_E when gradient correction is activated as compared to when it is not.

V. Discussion and Conclusions

The results presented from experiments in the Keck powered magnet at 25 T and in the 7.1 T superconducting magnet validate the effectiveness of the gradient correction control system implemented in tandem with the cascade field regulation system. This shows that the application of the gradient correction scheme significantly reduces the effect of gradient signals on the the inner loop controller, and allows the outer loop controller to work without error. Together, the systems are able to reduce field variations by about 38 dB, while reducing distortion in the spectral lineshape, which may facilitate the use of pulsed field gradients in powered magnets for high resolution MR experiments.

The control strategy presented in this work does possess several limitations. The chief limitation is that the relationship between input gradient signals and the output of the inductive measurement system is assumed to be linear. Part of the inductive measurements system is an integrating pre-amplifier, which can be pushed to non-linearity if the input gradient signal is not small enough. Fortunately, most classes of MR experiments do not require gradient strengths outside of the linear region. Secondary limitations include limits feedforwar filter complexity imposed by computational speed, and incomplete cancellation due to asynchronous sampling.

The impact of these limitations can be reduced by using more powerful hardware and software tools. Continued work with these tools is already underway on the 36 T SCH magnet.

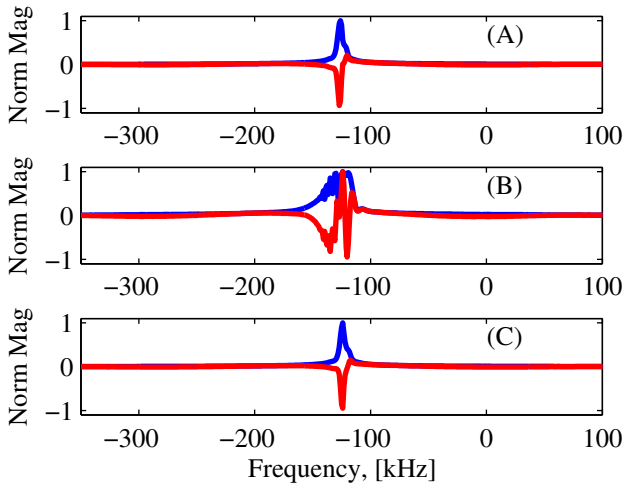

Fig. 13. Gradient augmented NMR excitation lineshape in the Keck powered magnet at 25 T with (A) no regulation (B) inner loop regulation with no gradient correction and (C) inner loop regulation with gradient correction.

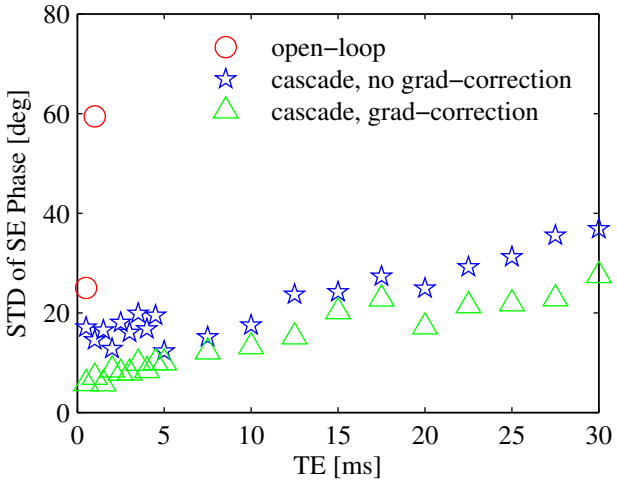

Fig. 14. Standard of Deviation of Spin Echo Phase with gradients with powered magnet disturbance applied for long T_E values.

VI. Acknowledgements

This work was supported by the US National Science Foundation and the state of Florida through NSF Cooperative Agreement DMR-0654118. This work was also supported in part by NSF Grants DMR-0603042 and DMR-1039938, and by NIH/NIGMS Grant P41 GM122698. The authors are grateful for developments on the field estimation and regulation system by Brian F. Thomson and Kiran K. Shetty. We also thank Mark D. Bird, Timothy A. Cross, Samuel C. Grant, James A. Powell, Peter L. Gor'kov, Zhehong Gan, Jason Kitchen and many others at the NHMFL who have contributed to the development of high resolution NMR in powered magnets.

References

[1] B. Shapira, K. Shetty, W.W. Brey, Z. Gan, L. Frydman. Single-scan 2D NMR spectroscopy on a 25 T bitter magnet. *Chemical Physics Letters* 442 (2007) 478-482.

[2] M. Li, J.L. Schiano, J.E. Samra, K.K. Shetty, W.W. Brey. Reduction of magnetic field fluctuations in powered magnets for NMR using inductive measurements and sampled-data feedback control, *Journal of Magnetic Resonance* 212 (2011) 254-264.

[3] B.D. McPheron, J.L. Schiano, B.F. Thomson, K.K. Shetty, W.W. Brey. Demonstration of 2D NMR spectroscopy in a powered magnet at 25 T using cascade field regulation *Proceedings of the 2019 American Control Conference* July 10-12, 2019.

[4] A. Kumar, D. Welti, R.R. Ernst. NMR fourier zeugmatography, *Journal of Magnetic Resonance* 18 (1975) 69-83.

[5] W.A. Edelstein. Spin warp NMR imaging and applications to human whole-body imaging, *Phys. Med. Biol.* 25 (1980) 751-756.

[6] R.E. Hurd. Gradient-enhanced spectroscopy, *Journal of Magnetic Resonance* 87 (1990) 422-428.

[7] J. Keeler, R.T. Clowes, A.L. Davis, E.D. Laue. Pulsed-field gradients: theory and practice. *Methods in Enzymology* 239 (1994) 145-207.

[8] M.D. Bird, W.W. Brey, T.A. Cross, I.R. Dixon, A. Griffin, S.T. Hannahs, J. Kynoch, I.M Litvak, J.L. Schiano, J. Toth, Commisioning of the 36 T Series-Connected Hybrid Magnet at the NHMFL, IEEE Trans. Appl, Supercond. 28, 3, 4300706 (2017).

[9] L. Ljung. System Identification Theory for the User. 2nd ed. *Prentice Hall* (1999)